WATER RESOURCES RESEARCH, VOL. 35, NO. 12, PAGES 3905–3917, DECEMBER 1999

Tidal networks
2. Watershed delineation and comparative network morphology

Andrea Rinaldo,[1] Sergio Fagherazzi,[2] Stefano Lanzoni, and Marco Marani
Dipartimento di Ingegneria Idraulica, Marittima e Geotecnica, Università di Padova, Padua, Italy

William E. Dietrich
Department of Geology and Geophysics, University of California, Berkeley

Abstract. Through the new method for automatic extraction of a tidal network from topographic or bathymetric fields described in a companion paper [*Fagherazzi et al*., this issue], we analyze the morphology of aggregated patterns that we observe in nature in different tidal environments. Specifically, we define, on the basis of a hydrodynamic analysis, a procedure for watershed delineation and for the identification of the "divides" for every subnetwork and look at the resulting drainage density and its related scaling properties. From the systematic, large-scale plots of drainage density and channel width versus watershed area we address the issue of a possible geomorphic criterion that corresponds to the parts of the tidal landscape that are characterized by river-like features. We also analyze the relationship of total contributing tidal basin area to channel widths and to mainstream lengths (Hack's law). We study comparatively probability distributions of total drainage areas and of "botanical" mass (the area of the channelized landscape upstream of a given section) for tidal and fluvial patterns and find altered scaling features of tidal landforms that reflect the complex interactions of different mechanisms that shape their geometry. Simple geomorphic relationships of the types observed in the fluvial basin (e.g., power laws in the watershed area versus drainage density, mainstream length, or channel width relationships) do not hold throughout the range of scales investigated and are site-specific. We conclude that tidal networks unlike rivers exhibit great diversity in their geometrical and topological forms. This diversity is suggested to stem from the pronounced spatial gradients of landscape-forming flow rates and from the imprinting of several crossovers from competing dynamic processes.

1. Introduction

In this paper, the second in a series of three, we quantify various tidal network properties including common power law relationships which have been well documented for terrestrial river systems [*Rodriguez-Iturbe and Rinaldo*, 1997]. Our goals here are both to explore tidal channel scaling properties and to infer, based on scaling breaks, possible changes in dominant formative process through a network. We anticipate that spatial variation in the dominance of ebb versus flood tides and in erosional resistance associated with vegetation and sediment texture could give rise to limited scaling compared to that found in terrestrial systems (where single power law relationships typically apply across many orders of magnitude). Hence we propose to apply common power law relationships quantified for terrestrial systems to tidal systems and use these analyses to identify possible geomorphic "signatures" of dominant processes.

Numerous studies have documented that the network of channels which develops across the tidal basin controls the hydrodynamics and sediment exchanges between salt marshes and tidal flats [e.g., *Pestrong*, 1965; *Boon*, 1975; *Pethick*, 1980; *Boon and Byrne*, 1981; *Speer and Aubrey*, 1985; *Friedrichs and Aubrey*, 1988; *Parker*, 1991; *Friedrichs and Madsen*, 1992; *Friedrichs*, 1995; *Steel and Pye*, 1997]. Fewer studies have examined scaling properties, with the recent paper by *Steel and Pye* [1997] being a notable exception. Although Steel and Pye rely on a Horton morphometric analysis, which generally is unable to identify differences between networks [e.g., *Kirchner*, 1993; *Rinaldo et al*., 1998], they do report differences between tidal and fluvial network forms. *Steel and Pye's* [1997] analysis was also limited in its overview of the role and form of tidal networks.

In order to perform morphometric analysis of tidal networks, we need an objective procedure for delineating the drainage area to any link. Here we first introduce a new method, based on flow hydrodynamics, for delineating drainage directions and contributing areas throughout the tidal network. We then apply this method to the three tidal basins used in the previous (part 1) paper: northern part of the Venice Lagoon, Petaluma Marsh in San Francisco Bay (California), and the great marshes at Barnstable (Massachusetts). This then enables us to compare scaling relationships in tidal networks with those found in fluvial systems [e.g., *Rodriguez-Iturbe and Rinaldo*, 1997]. Instead of finding scale invariance tendencies so prevalent in fluvial systems, our analyses reveal a complete lack of such tendencies in tidal channel systems.

[1]Also at Ralph M. Parsons Laboratory, Massachusetts Institute of Technology, Cambridge.
[2]Now at Computational Science and Engineering Program, Florida State University, Tallahassee.

Paper number 1999WR900237.
0043-1397/99/1999WR900237$09.00

2. Watershed Delineation in Tidal Basins

Watershed delineation for a tidal channel has theoretical and practical difficulties. First of all, ebbing and flooding phases preclude the definition of a divide as a time-independent locus of points in space. One also wonders whether the assumption that maximum discharge is proportional to upslope contributing area (on which several geomorphological relationships hinge [e.g., *Myrick and Leopold*, 1963; *Leopold et al*., 1984, 1993; *Collins et al*., 1987]) holds in tidal basins. If the time of propagation of the tidal wave over the network is negligible with respect to the period of the forcing tides, one surely expects such a relationship to hold. Hence it would hold for quasi-static sublagoons where the relatively fast time of wave propagation produces a nearly horizontal fluctuation in water level through time across the entire tidal embayment, but many more cases of interest are conceivable. Thus watershed delineation is deemed important.

In tidal basins, drainage directions should be defined by the steepest descent of the water surface topography. This topography, however, varies with time and in space and is governed by the momentum and mass balance equations which, usually, assume a two-dimensional form owing to the shallow depth usually encountered in tidal embayments. We propose that flow directions can be defined by the solution of the following mathematical problem. Let Γ be the domain of tidal flow expansion and let $\partial\Gamma(\mathbf{x})$ be the spatial location of its boundaries, that is the spatial position of the channel network, identified in this case (but not necessarily) by the procedure defined by *Fagherazzi et al*. [this issue]. We assume that tidal propagation within the creek network is instantaneous compared to that on the shallow salt marshes or flats. This implies that the celerity of tidal wave propagation (which is, to first order in both cases, proportional to $\sqrt{gD_0}$, where D_0 is the mean flow depth) is much larger in the channels than in the shallow flats (see section 2 of *Rinaldo et al*. [this issue]). We also assume that such propagation across the shallow flats is dominated by hydraulic resistances; that is, friction terms dominate inertial effects in momentum equations. Under such limiting conditions one can simplify the governing equations (see the Appendix), obtaining a dimensionless Poisson form within Γ:

$$\nabla^2\eta_1(\mathbf{x}, t) = \frac{\Lambda}{\eta_0^2}\frac{\partial\eta_0}{\partial t} \tag{1}$$

and on $\partial\Gamma(\mathbf{x})$

$$\eta_1(\mathbf{x}, t) = 0, \tag{2}$$

where Λ is an effective dimensionless friction coefficient and η_0 and η_1 are defined in Figure 1. Notice that in Figure 1 an asterisk denotes dimensional quantities (see the Appendix) and that (2) reflects the much faster propagation of the tidal wave within the deep channels than across the shallow flats. We further assume the forcing right-side term of (1) to be constant, say K, thereby neglecting the rate of change of the average water level η_0 and allowing us to assume that there are negligible gradients of mean flow depth across the marsh plain. Thus the above boundary value problem is modified by the new version of (1):

$$\nabla^2\eta_1 = K, \tag{3}$$

which is valid within the tidal expansion domain Γ.

Needless to say, the above mathematical formulation of the problem is a highly simplified one and is applicable, in principle, only for relatively short, nearly flat tidal expansions with a well developed and deep channel network (where, for dynamic reasons [e.g., *Dronkers*, 1964], the celerity of the tidal wave may be slightly reduced by storage effects but maintains a relatively high value proportional to $\sqrt{gD_0}$, where D_0 is the mean depth of the channel). However, the potential field $\eta_1(\mathbf{x})$ thus determined allows the computation of drainage directions $\nabla\eta_1(\mathbf{x})$ which we assume to be substantially time-invariant. From these data one can determine the "watershed" of a cross section by finding the set of pixels connected to that site through a downhill (of the water surface) steepest descent. Hence one can calculate watershed boundaries just from the mapped position of the tidal channels (i.e., by assuming the right-side term in (3) equal to $K = 1$, one needs no bathymetric information to compute the surface elevation field $\eta_1(\mathbf{x})$ and its related gradients $\nabla\eta_1(\mathbf{x})$). In the actual computations we use the fast and efficient numerical solution developed for arbitrary domains by *Marani et al*. [1998].

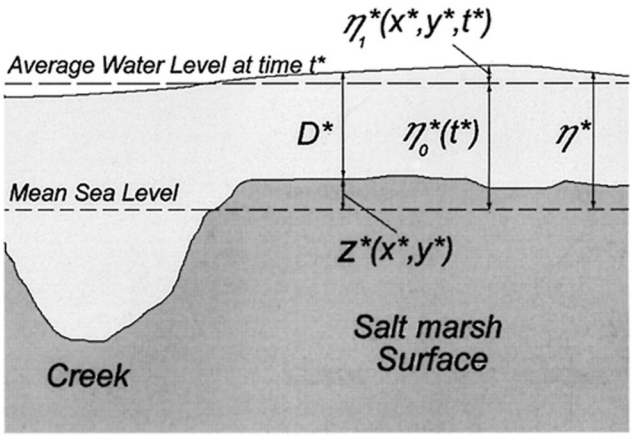

Figure 1. Notation as follows: η^* is the tidal elevation, which can be divided into η_0^*, average tidal elevation in the basin at time t^* and η_1^*, local surface elevation above η_0, D^* is water depth on the salt marsh, and z^* is the bottom elevation referenced to the mean sea level.

One example of watershed delineation for the planar field of Petaluma Marsh [*Fagherazzi et al*., this issue, Figure 3] is described in Figures 2 and 3. Figure 2 shows the surface elevation field produced by solving the mathematical problem ((3) with boundary conditions given by (2)) in the geometry of that site. Figure 3a shows a subset of the steepest descent directions associated with the field of free surface elevations shown in Figure 2. Figure 3b shows four watersheds delineated through the steepest descent direction of the water surface landscape shown in Figure 2, identified within the area shown in Figure 3. The particular watersheds shown are arbitrarily chosen for clarity at the outlets to larger channels.

Next we use the drainage areas calculated by this procedure to explore scaling relationships in our tidal networks. In the third paper of this series [*Rinaldo et al*., this issue] we exploit this ability to delineate flow directions to simplify greatly the modeling of flow through the tidal network.

3. Scale Dependence and Scale Invariance in Tidal Networks

In fluvial studies, drainage density, traditionally defined as the ratio of total network length to watershed area, for exam-

Figure 2. The vertically exaggerated water surface topography derived from solving equation (3) by assuming $K = 1$ for the Petaluma Marsh study area (depicted in Figure 3 of *Fagherazzi, et al*. [this issue]). The choice of the constant K is immaterial for the delineation of drainage directions because of the linearity of the mathematical solution. Notice the membrane-like features of the potential field that uniquely define drainage directions.

ple, measured per meter, measures the degree of dissection of a watershed by streams, and its inverse is proportional to the distance one has to walk, on average, before encountering a channel. The concept of drainage density implies the existence of a fundamental length scale associated with the dissection of the landscape by the river network [e.g., *Montgomery and Dietrich*, 1992].

In tidal basins the nonnegligible size of the channels with respect to the system size and the varying textures encountered suggest the introduction of alternative measures of drainage density, reflecting both the typical flow length in unchanneled areas and the extent of channeled basin areas to total area. We thus first define a parameter D_1, a drainage length, defined as the ratio of the total basin area to the total network length, here measuring the length of the skeleton of the network [see *Fagherazzi et al*., this issue, Appendix]. D_1 is a dimensional quantity (a length) measured in meters. Physically, D_1 is an estimate of the average unchanneled distance and is the inverse of the drainage density as usually defined in fluvial studies. Second, we define a parameter D_2, a channel area proportion, defined as the ratio of channeled area (the total number of channelized pixels [*Fagherazzi et al*., this issue]) to the total basin area (the total number of pixels within the watershed). It is a dimensionless number $0 \leq D_2 \leq 1$ that physically represents the fraction of the tidal embayment occupied by the channels.

Figures 4 and 5 illustrate the results of the application of the above definitions, through the techniques to extract geometrical information described by *Fagherazzi et al*. [this issue], to four different tidal environments: Petaluma Marsh (California), Barnstable Marsh (Massachusetts), a small salt marsh zone within the Venice Lagoon (Pagliaga salt marsh), and the entire channelized part of the northern lagoon of Venice. For selected intervals of watershed area (which are multiples of the pixel size) the mean and variance of D_1 and D_2 were calculated and plotted against the corresponding logarithm of watershed area. The lack of variance in the larger areas reflects the fewer samples obtained. Values of D_1 tended toward constant values for ~2–4 orders of magnitude of drainage area in three of the four cases, whereas only in Barnstable Marsh did D_2 show any tendency toward a constant value at all scales.

Hack's [1957] law is an empirical relationship that relates, within a river basin, total contributing area A to mainstream length, say L. Here L is computed by counting the number of pixels along the skeleton of the network [*Fagherazzi et al*., this issue] following the channel with largest contributing area up to the watershed divide. In fluvial systems, Hack's law maintains a noteworthy consistency through many scales as a power law of the type $L \propto A^{0.57 \pm 0.03}$ [see, e.g., *Rodriguez-Iturbe and Rinaldo*, 1997]. The significant departure from an exponent of 0.5, which would have characterized a Euclidean mathematical object [*Mandelbrot*, 1982], has attracted considerable interest

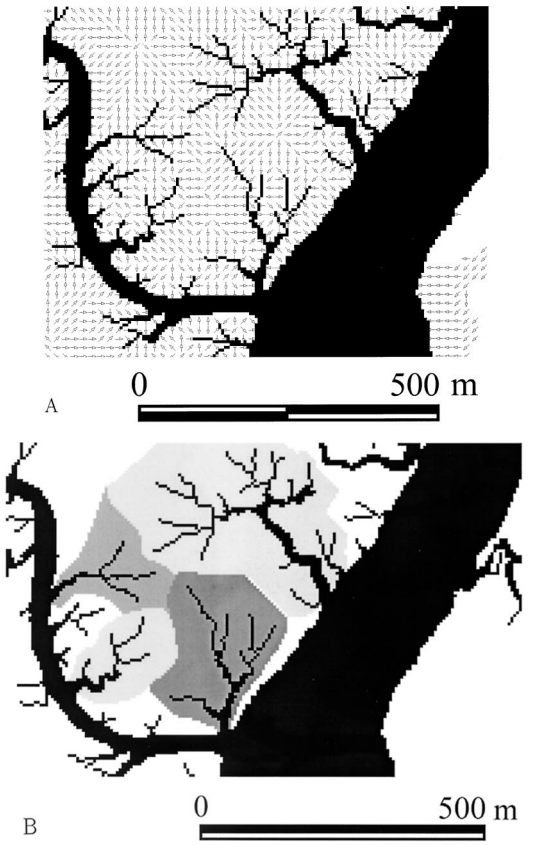

Figure 3. Examples of flow direction and resulting watershed delineations for a subarea of the Petaluma Marsh. (a) Plot of directions of steepest descent associated with the free surface depicted in Figure 2. A small subset (of the order of 500×500 m^2) is selected for clarity. (b) Delineation of four tidal basins, each one shown in different degrees of shading, which join a major channel. For clarity other basins are not depicted.

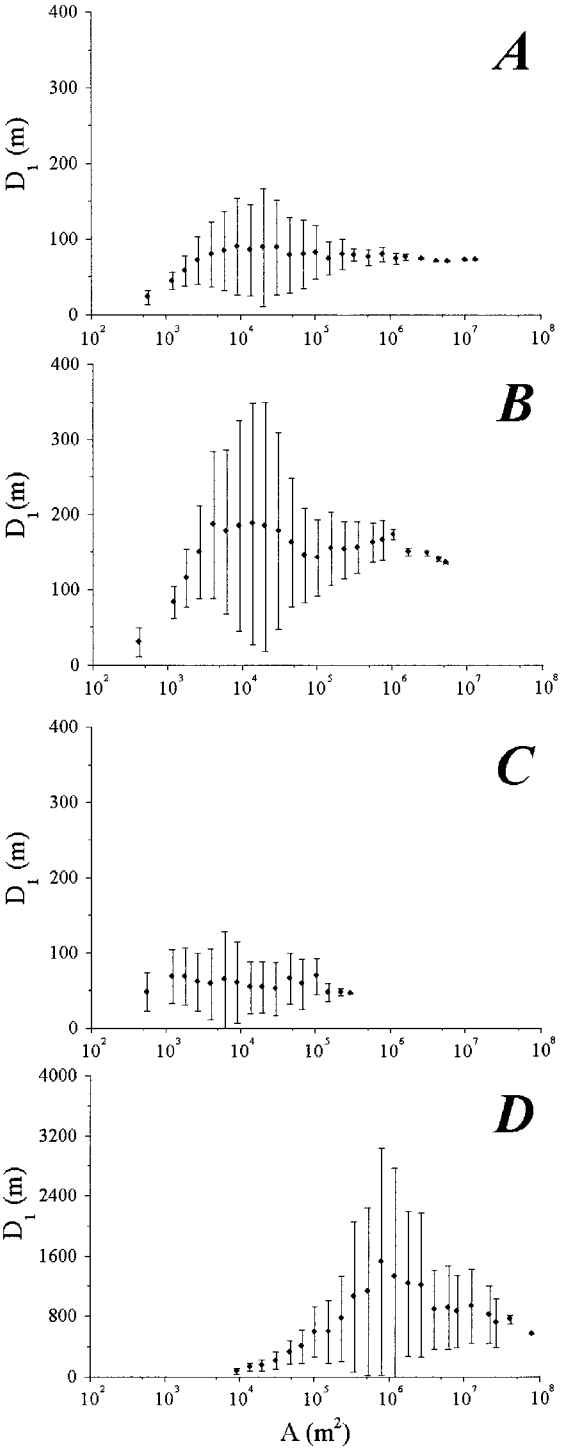

Figure 4. Mean and variance of the drainage density parameter D_1 (meters) versus total watershed area A (square meters) of a large number of watersheds within the tidal basins studied, delineated as shown in Figure 2. The semilogarithmic plots emphasize the mean values (expected value from the distribution inferred from the samples of drainage density given the network area) and the estimated variance. Network lengths needed to obtain values of D_1 are computed by extracting the skeleton [*Fagherazzi et al*., this issue] and measuring its total length: (a) Petaluma Marsh (California); (b) Barnstable Marsh (Massachusetts); (c) Pagliaga salt marsh within the Venice Lagoon; and (d) the entire channelized pattern of the northern part of the Venice Lagoon.

from geomorphologists [e.g., *Hack*, 1957; *Gray*, 1961; *Muller*, 1973; *Montgomery and Dietrich*, 1992] and in fractal studies, especially through finite-scale scaling arguments [e.g., *Rigon et al*., 1996]. Figure 6 shows the area-mainstream length (log-log) plots for the same networks employed for the study of drainage densities (Figures 4 and 5). Mean values, that is, ensemble averages of area given mainstream length, are also shown. All of the plots of length against slope are curved unlike the power law relationship found in fluvial systems. Power law fits were made just to longest straight portions of the graphs.

The geomorphological width function, say $W(x)$, is defined as the relative proportion of contributing area a given length x from the outlet of the basin, the length being measured along the channel path. Width functions are useful in fluvial hydraulics because they are dynamically related to the isochrones of travel time [*Kirkby*, 1976] and may be used to describe the effect of the interplay of hillslope and fluvial domains on the hydrologic response [*Rinaldo et al*., 1995]. Figure 7 shows one example of width function computed for tidal networks. Technically, the width function is computed as follows. For every pixel one computes its along-stream distance to the outlet, here following the procedure described by *Fagherazzi et al*. [this issue]. We then divide the network into sets of connected points whose distance from the outlet lies in the interval $d \leq$

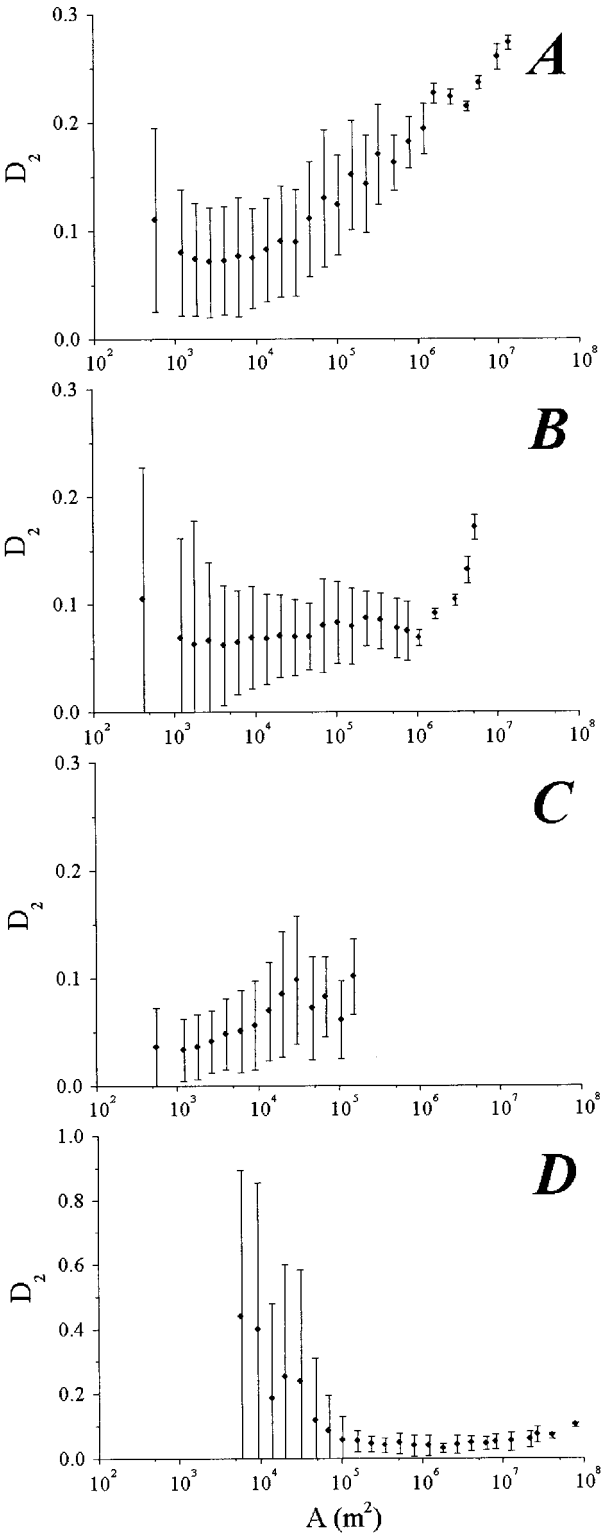

Figure 5. Mean and variance of the dimensionless drainage density parameter D_2, defining the relative proportion of unchanneled tidal areas versus total area A for a large sample of individual watersheds delineated as shown in Figure 2. Values of D_2 are computed by counting the number of channeled pixels [*Fagherazzi et al.*, this issue]: (a) Petaluma Marsh (California), (b) Barnstable Marsh (Massachusetts), (c) Pagliaga salt marsh within the Venice Lagoon, and (d) the entire channelized pattern of the northern part of the Venice Lagoon.

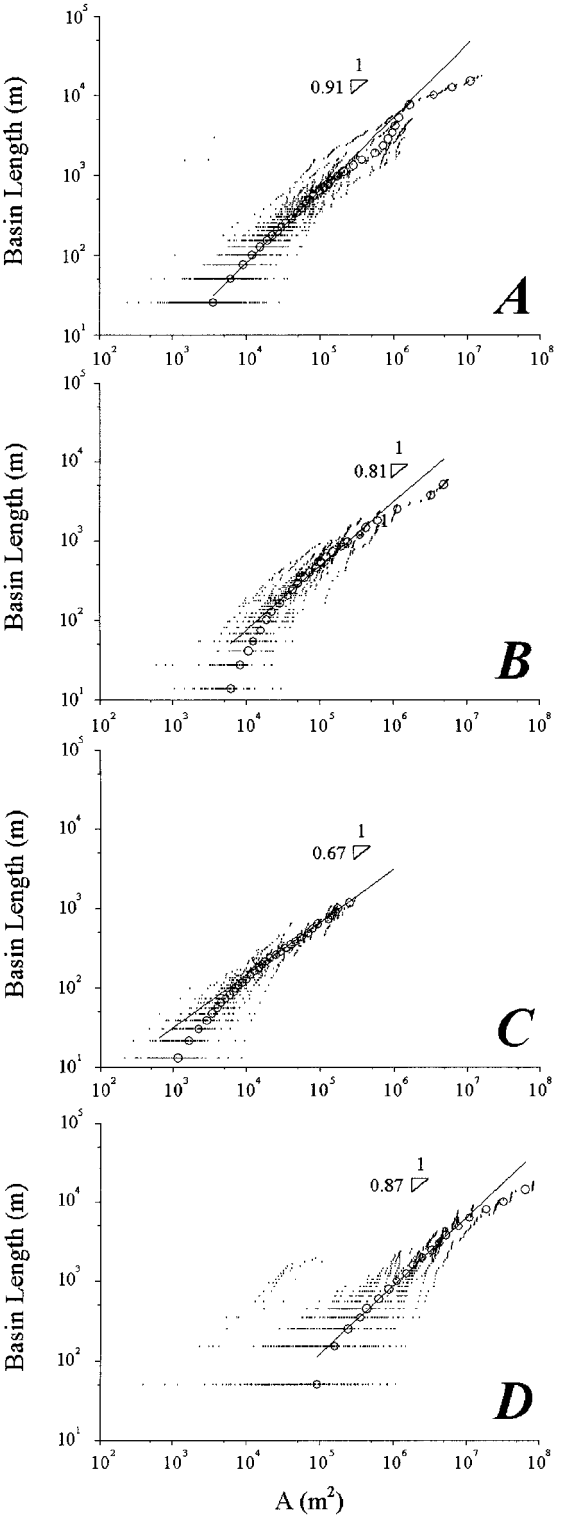

Figure 6. Mainstream length of tidal subbasins versus total basin area: (a) Petaluma Marsh (California), (b) Barnstable Marsh (Massachusetts), (c) Pagliaga salt marsh within the Venice Lagoon, and (d) the entire channelized pattern of the northern part of the Venice Lagoon. Notice that lengths are computed using the identification techniques described by *Fagherazzi et al.* [this issue]. The larger open circles represent the ensemble mean (mean drainage area given the mainstream length). Slopes are fitted to the scaling of mean values through selected portions of the graphs, that is, whenever reasonable.

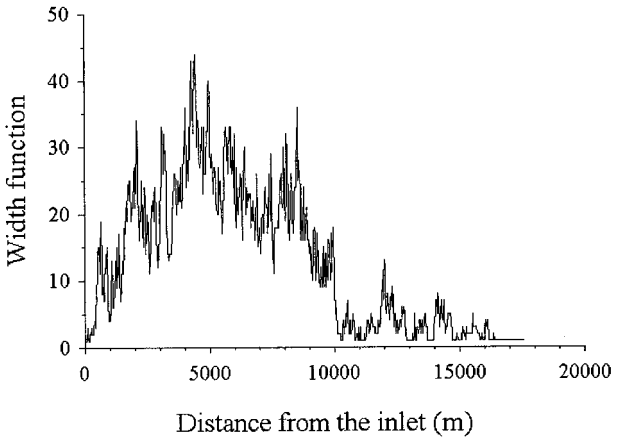

Figure 7. The width function of the tidal network identified within the Pagliaga salt marsh in the northern part of the Venice Lagoon. Along-stream distances x are measured in pixels (each pixel side measures 10 m), and the width function $W(x)$ counts the number of pixels placed at distance x from the outlet.

$x \leq d + k$ and define their overall distance as the value $d + k/2$. The width function is the number of set points having the same distance to the outlet. Power spectra have been used [e.g., *Marani et al*., 1994] to study recurrent features of width functions of fluvial basins as they describe their broad structure. Figure 8 shows the power spectra of the width functions obtained for the entire lagoon of Venice and Barnstable and Petaluma marshes.

In fluvial basins it is commonly assumed that total contributing area A is proportional to landscape-forming discharges Q. This assumptions is reasonable whenever the basin dimension does not exceed a scale characteristic of the heterogeneity of meaningful spatial patterns of intense rainfall, and this is commonly assumed to hold for several orders of magnitude. In tidal networks one faces the challenge of the interaction of ebb and flood flows in shaping the morphology of the network, and thus we wonder whether watershed areas have as strong a morphodynamic meaning. In particular, the relationship between channel width and basin area is likely to be strongly affected by the very rapid along-stream changes typical of tidal estuaries [*Leopold et al*., 1984, 1993; *Myrick and Leopold*, 1963] and by the complex dynamics of water storage exchange with the marsh and tidal flats.

In Figure 9 the watershed area, computed by the method described in this paper, is plotted as a function of channel width (determined by the procedure described in paper 1 [*Fagherazzi et al*., this issue]). The data were binned by intervals of width, and the mean area for each bin category is also plotted. Power law fits were made to the relatively linear portions of each plot, and the resulting exponents differ markedly among the sites.

The most important signatures of scale-invariant processes acting in the tidal basins are related to the existence of power law characteristics in the tails of probability distributions of relevant geometrical quantities. We have studied four indicators. Figures 10a–10d show a double logarithmic plot of the exceedence probability of watershed area, $P(A \geq a)$ plotted against area a (here the upper case denotes the random variable and the lower case denotes the current value in square meters) for the four field cases, that is, Petaluma Marsh, Barnstable Marsh, the Pagliaga salt marsh, and the northern part of the Venice Lagoon. For the same environments, Figures 11a–11d show the exceedence probability of total network length, measured upstream of each site. The latter is an interesting measure that, in river networks, defines Hortonian ratios of bifurcation and length [*Tarboton et al*., 1988; *Rodriguez-Iturbe and Rinaldo*, 1997]; Figures 12a–12d show the exceedence probability of tidal channel cross-section width, measured via the algorithm described by *Fagherazzi et al*. [this issue]. Its statistics are important since width is functionally related to the landscape-forming flow rates [*Myrick and Leopold*, 1963]; Figures 13a–13d show the distribution of the exceedence of the "botanical" mass of the tidal tree. Mass is computed by measuring the planimetric area occupied by the channels above a given section, which is roughly equivalent to the mass or weight of a tree cut at any section. All four indicators plot as curved lines rather than well-defined power law relationships, suggesting a distinct lack of scaling in tidal systems.

Finally, an important geomorphological attribute is the condition associated with tidal channel initiation, as this controls the drainage density. In fluvial basins [*Montgomery and Dietrich*, 1988, 1992] it is dictated by a threshold which includes both total contributing area and slope. Figure 14 shows the distribution of watershed area at the initiation of tidal channels within the Petaluma Marsh (Figure 14a) and within the Barnstable great marsh (Figure 14b). Both basins show a peak of channel initiation at ~500–1000 m^2.

4. Discussion

Drainage spacing properties, illustrated by parameters D_1 and D_2, are varied both across individual basins and between

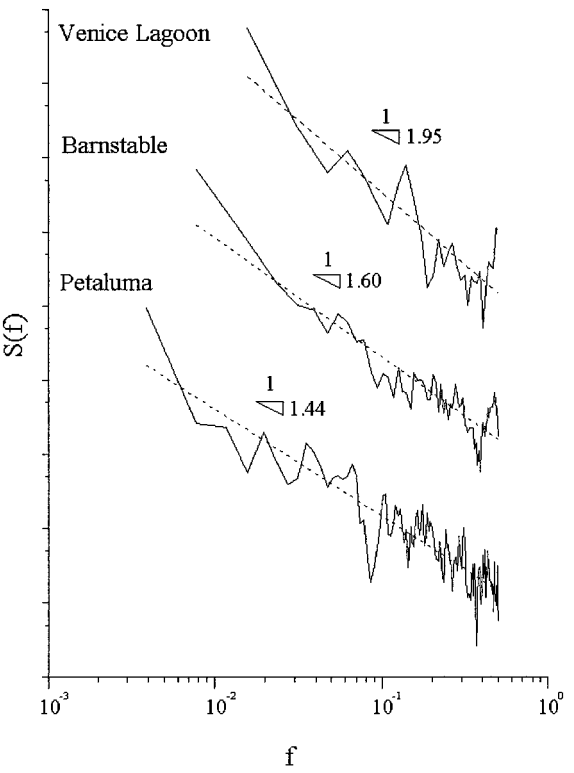

Figure 8. Power spectra of the width functions $W(x)$ of the network of the northern part of Petaluma Marsh, Barnstable Marsh, and the Venice Lagoon.

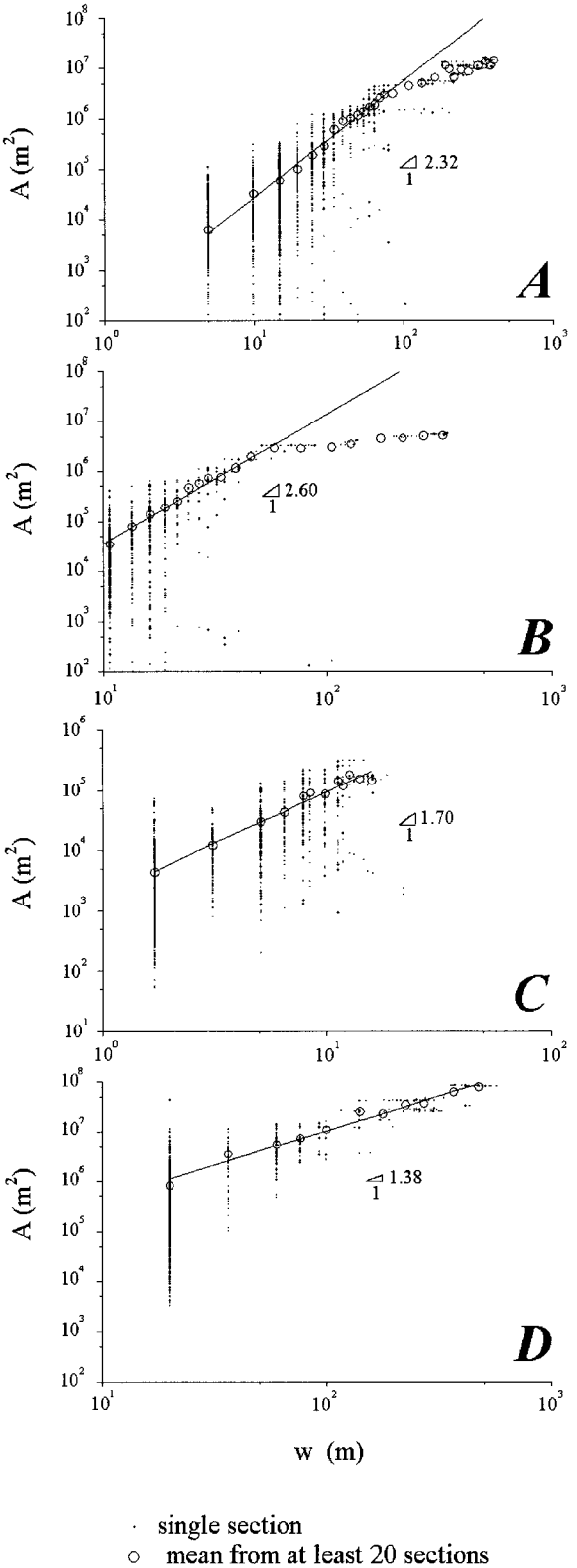

Figure 9. Watershed area A versus cross-section width w computed for the four tidal environments: (a) Petaluma Marsh, (b) Barnstable Marsh, (c) Pagliaga salt marsh, and (d) Venice Lagoon of Figure 4. A dot represents the value corresponding to a single cross section, while a circle indicates the ensemble mean from at least 20 sections.

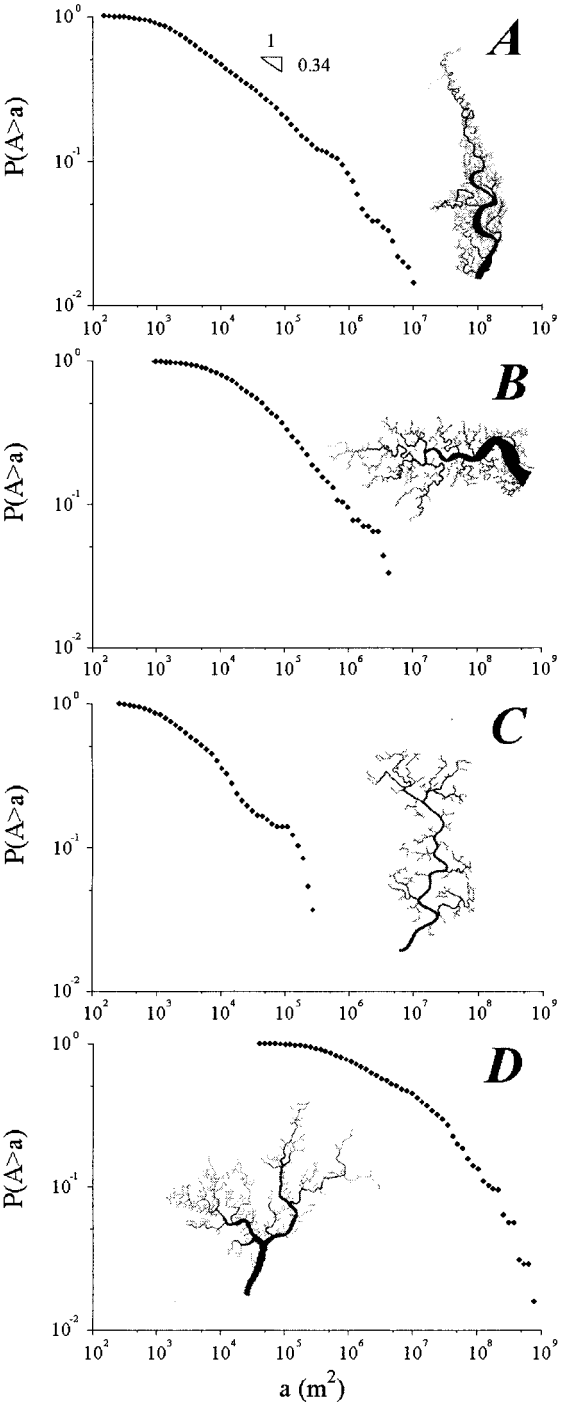

Figure 10. Double logarithmic plot of the exceedence probability of watershed area $P(A \geq a)$ (versus the current value of area a) computed for the four tidal environments (a) Petaluma Marsh, (b) Barnstable Marsh, (c) Pagliaga salt marsh, and (d) Venice Lagoon of Figure 4.

sites. While in some cases the parameter D_1 is highly variable and mostly scale-dependent, in others it shows more stable and converging features. Channel networks on the Petaluma Marsh (Figure 4a) rapidly converge to a drainage length D_1 of about 100 ± 50 m which persists for about 3 orders of magnitude of drainage area. Barnstable networks (Figure 4b) have greater variance, that is, $< D_1 > \approx 150 \pm 100$ m, even when the

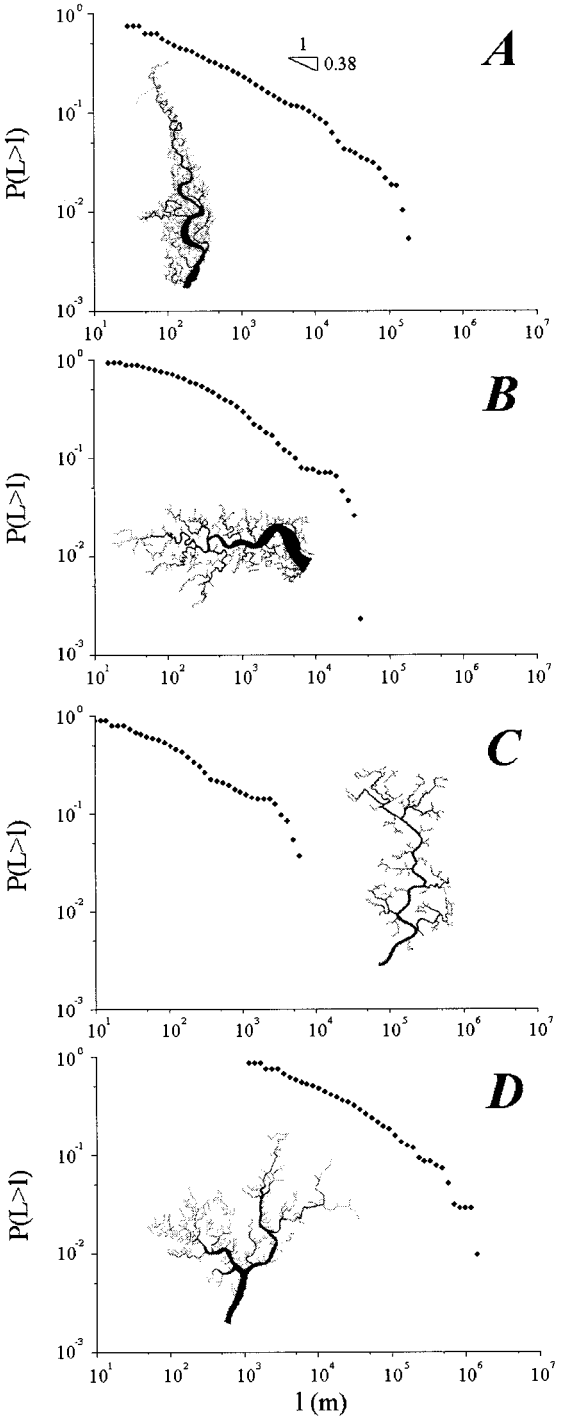

Figure 11. Double logarithmic plot of the exceedence probability of lengths L to the divide $P(L \geq l)$ (versus the current value of length l in meters), computed for the four tidal environments (a) Petaluma Marsh, (b) Barnstable Marsh, (c) Pagliaga salt marsh, and (d) Venice Lagoon of Figure 4.

sample size is large (such as occurs for drainage areas of 10^5 m^2). The lagoon of Venice (Figures 4c and 4d) is spatially heterogeneous. The small salt marsh of Pagliaga (Figure 4c) has small distances ($D_1 \sim 70 \pm 50$ m) and thus large drainage densities, which remain relatively constant over a small range of areas. The larger lagoon shows larger and more variable lengths. In fact, D_1 is about an order of magnitude larger than that in Pagliaga (i.e., about 1000 m) and does not converge. The larger lagoon pixel size is 20 m (as compared to 1 m for Pagliaga and 20 m for Petaluma and Barnstable); hence it cannot have drainage lengths as small as Pagliaga. Furthermore, significant portions of the larger lagoon are composed of unchanneled mud flats and indistinct lowlands. These unchanneled areas may be a consequence of the radical changes in

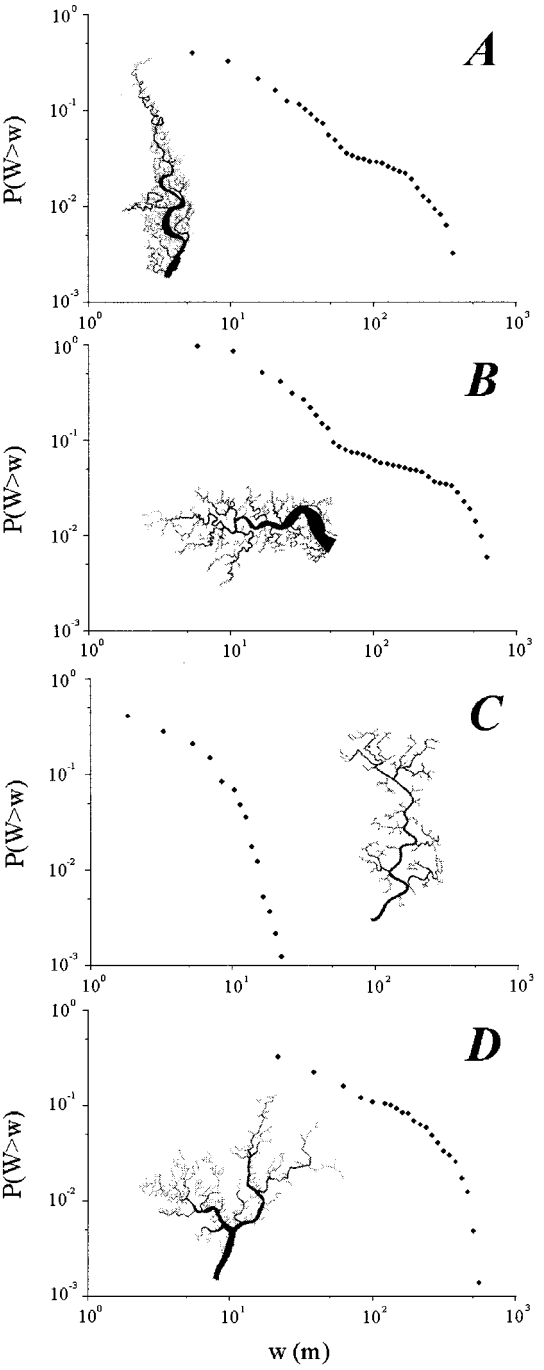

Figure 12. Double logarithmic plot of the exceedence probability of channel width w area $P(W \geq w)$ (versus the current value w in meters), computed for the four tidal environments (a) Petaluma Marsh, (b) Barnstable Marsh, (c) Pagliaga salt marsh, and (d) Venice Lagoon of Figure 4.

sediment inflows associated with river diversions for the past several hundred years.

The related plot of the channel area proportion (D_2) shows different trends (Figure 5). Petaluma's D_2 is relatively stable at about 0.08 $\pm$ 0.05 for areas draining about 10^3 to 10^4 m^2 but then increases steadily with increasing areas to a value close to 0.25. Barnstable Marsh (Figure 5b) has a roughly constant value of D_2 of less than about 0.1 up to about 10^6 m^2. In contrast, the large size of the channels close to the mouths in the lagoon of Venice causes D_2 to approach a constant there. The wide variance of D_2 for areas of 10^4 to 10^5 m^2 results from the extensive unchanneled tidal flats in the central lagoon.

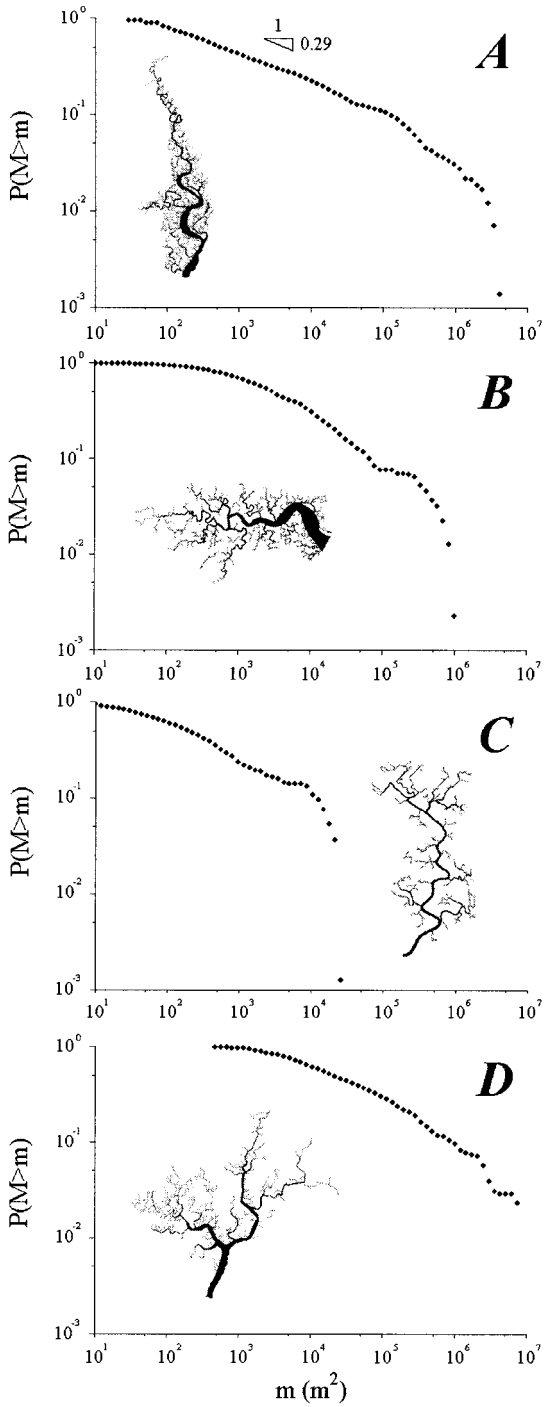

Figure 13. Double logarithmic plot of the exceedence probability of botanical mass M area $P(M \geq m)$ (versus the current value m expressed in square meters), computed for the four tidal environments (a) Petaluma Marsh, (b) Barnstable Marsh, (c) Pagliaga salt marsh, and (d) Venice Lagoon of Figure 4.

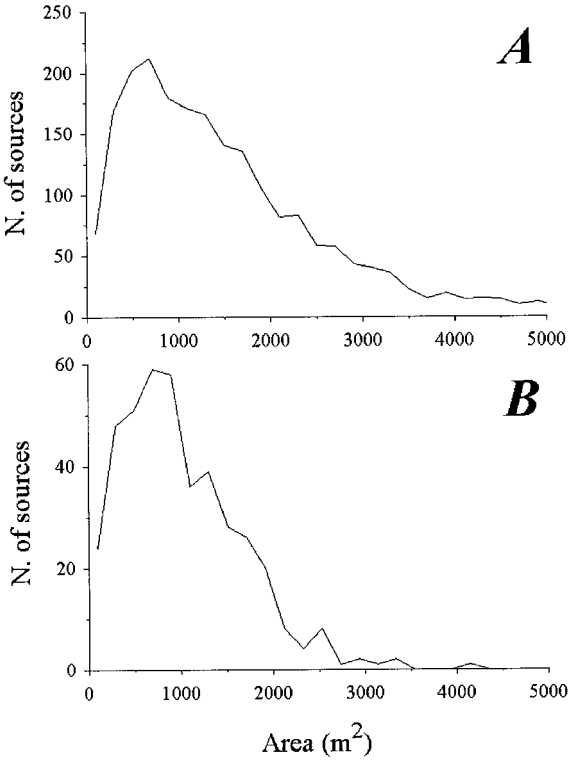

Figure 14. Probability density function of watershed area at channel initiation for (a) Petaluma Marsh and (b) Barnstable Marsh.

Hack's law (Figure 6) does not seem to apply to tidal networks. In stark contrast to fluvial systems where the exponent of the power dependency of area on length consistently falls between 0.54 and 0.6 for individual basins [e.g., *Rodriguez-Iturbe and Rinaldo*, 1997], in our tidal networks no single power law was applicable across a wide range of the data. Furthermore, when we fit a power law to the most linear portions of each data set, we found that the exponents differed greatly among basins and with that found in fluvial systems.

The width function is a broad measure of spatial organization of the network, and *Marani et al.* [1994] have found that the slope of the power spectra of the width function in fluvial systems has small variance. In contrast, we find that the spectra slopes differ widely among Petaluma Marsh, Barnstable Marsh, and Venice Lagoon. Again, this suggests that network aggregation in tidal systems is fundamentally different from that found in fluvial networks.

Consistent with the other measures, the four probability distributions (Figures 10–13) also lacked scale-invariant power law distributions. Only the smaller areas of Petaluma Marsh showed a tendency for scaling. For example, the area distribution (Figure 10) could be defined by the relationship $P(A \geq a) \propto a^{-0.34}$ between about 10^3 and 10^5 m^2 drainage area. This scaling exponent is significantly different from that usually found for river basins (which lies in the range of 0.41 to 0.45) [*Rodriguez-Iturbe and Rinaldo*, 1997].

Perhaps most surprising, for two of the basins (Petaluma and

Barnstable) even the power law relationship between drainage area and channel width had significant breaks in them. These breaks are obvious from visual inspection of the plan maps of the basin where one can see that the mainstem of each network experiences vary rapid widening (compared to the increasing drainage area) as the basin mouth is approached (see insets in Figures 10a and 10b).

Taken together, these various measures of network properties show a nearly complete lack of scaling in our tidal networks. For individual measures, however, portions of the network appear to show some scale invariance, and we attempted to see whether for these portions, a common scale invariance could be found across the various measures employed. We did this by looking at where approximate breaks in the scaling could be identified. For example, in the Petaluma basin, drainage properties showed breaks at drainage areas (square meters) of 10^4 for both D_1 and D_2 but at about 2×10^5 for Hack's law and 2×10^6 for channel width. In Barnstable these corresponding breaks occurred at about 5×10^3, 10^6, 2×10^4, and 2×10^6 m^2. In Pagliaga, no apparent break occurred for D_1 or for channel width, but distinct breaks occurred for D_2 at about 2×10^4 and for Hack's law at 10^4 m^2. Finally, in the coarser data set of the northern Venice Lagoon, breaks for D_1 and D_2 occurred at 10^6 and 10^5, respectively, where a break in Hack's law occurred at 10^7 m^2, but none occurred in the channel width relationship. We are forced to conclude that there is not a common scale break for individual basins where various network properties coincidentally change.

Breaks in power law relationships can be interpreted as reflecting a change in dominant formative process. There are many factors in tidal networks that should defeat scaling tendencies. The relative importance of ebb and flood flows in shaping channels probably varies from mouth to channel tip, with ebb flows possibly being more important in the smaller marsh flat channels. Vegetation and sediment texture which influence erosion and deposition processes may vary with channel scale and with relative height across the tidal basin. Tidal networks may preserve features associated with their evolutionary development from mudflats to marsh plain; that is, the flows responsible for network evolution may have become ineffective with marsh plain formation; hence some features of networks may be static legacies rather than dynamically shaped by current flows. Importantly, many tidal networks near populated areas have been altered for various practical purposes. Drainage channels have been cut for mosquito control. Bends have been cut off for navigation. In the case of our Venice Lagoon site, sediment inflows have been excluded through river diversion for several hundred years.

It is apparent that just as models of fluvial channel networks have sought to explain their pervasive scale-invariant properties, models of tidal network development will need to predict their scale-dependent character. In the third paper in this series we will introduce a new method for computing channel network flows which should form a foundation for a hydrodynamic investigation of the tidal network development.

5. Conclusions

We have studied the morphology of several tidal networks extracted from digital maps. We first defined watershed area for each cross section via a new procedure for watershed delineation, based on a simplification of the flow equations. The procedure is time-invariant and reduces to a Poissonian problem. We consequently studied important structural relationships related to watershed area, defined for the tidal basin and its networks: the variations of drainage density within the basin; Hack's relationship; the complex scaling of watershed area with channel width; the probability distributions for areas, lengths, widths and total mass; and tidal channel initiation. The comparison of similarities and departures among fluvial and tidal networks sheds light on the complex dynamic mechanisms producing scale invariance in nature and provides a tool for the validation of morphodynamic models. Whereas fluvial systems show various scale-invariant tendencies, there seems to be a nearly complete lack of such tendencies in tidal networks.

Appendix

Here we derive (3) of the main text, the solution to which enables us to delineate flow directions across the marsh plain to bounding channels and thereby delineate the watershed area to any channel cross section draining the marsh plain. This model, while physically based, only requires information on the spatial location of the channels and of the bordering mainland and salt marsh edge. By assuming a linear frictionally dominated flow across the marsh plain, we can calculate the local watersheds using the divergence of flow directions across the plain which results from curvature of the free surface of the flood waters. Although the location of local watershed divides will vary through the tidal cycle and with different tides, we purposely simplify the equations in order to define time-independent watershed areas which can then be useful in morphologic analysis. These simplifications make the model most valid for relatively short embayments, such that the water surface at any give time can be assumed to depart only slightly from a flat configuration. This assumption has been done in continuity models developed in the past [*Boon*, 1975; *Pethick*, 1980] and in recent approaches to basin morphodynamics [*Shuttelaars and Swart*, 1996; *Van Dongeren and De Vriend*, 1994].

The flow field in a tidal lagoon is described by the two-dimensional, depth-averaged equations of momentum and continuity which, assuming the Boussinesq approximation in the horizontal and the hydrostatic approximation in the vertical to be satisfied [*Dronkers*, 1964], yield

$$\frac{\partial U^*}{\partial t^*} + \left[U^* \frac{\partial U^*}{\partial x^*} + V^* \frac{\partial U^*}{\partial y^*} \right] = -g \frac{\partial \eta^*}{\partial x^*} - g \frac{U^*}{C^2 D^*} \cdot \sqrt{U^{*2} + V^{*2}} \tag{A1a}$$

$$\frac{\partial V^*}{\partial t^*} + \left[U^* \frac{\partial V^*}{\partial x^*} + V^* \frac{\partial V^*}{\partial y^*} \right] = -g \frac{\partial \eta^*}{\partial y^*} - g \frac{V^*}{C^2 D^*} \cdot \sqrt{U^{*2} + V^{*2}} \tag{A1b}$$

$$\frac{\partial}{\partial x^*} (D^* U^*) + \frac{\partial}{\partial y^*} (D^* V^*) + \frac{\partial D^*}{\partial t^*} = 0, \tag{A1c}$$

where (U^*, V^*) denote the depth-averaged flow velocities in the (x^*, y^*) directions, η^* denotes the height of the water with respect to the mean sea level, t^* denotes time, D^* is the flow depth, C, is Chézy's friction coefficient, and g is the gravitational acceleration (Figure 1).

Our main aim is to evaluate typical flow directions across the salt marsh when the maximum discharge occurs. This reportedly corresponds to the flow stage yielding maximum flood

velocity attained before high water, and this usually corresponds to over-bank spills onto the marsh surface [*Pethick*, 1980; *Healey et al*., 1981]. We then focus our attention on a neighborhood of this instant and consider the following decomposition of water depth:

$$D^*(x^*, y^*, t^*) = \eta_0^*(t^*) + \eta_1^*(x^*, y^*, t^*) - z^*(x^*, y^*), \quad \text{(A2)}$$

where η_0^* is the average tidal elevation on the salt marsh at time t^*, with respect to the mean sea level, z^* is the elevation of the salt marsh bottom referred always to the mean sea level, and η_1^* is the local water surface elevation above η_0^* (Figure 1).

We need now to estimate the relative importance of the various terms in the governing equations. To this purpose it is worthwhile to make dimensionless the relevant physical quantities as follows (here the dimensionless quantities retain the symbol used for corresponding dimensional counterparts with the asterisk removed):

$$(\eta_0^*, z^*) = D_0(\eta_0, z), \qquad \eta_1^* = a_0\eta_1$$

$$(U^*, V^*) = U_0(U, V), \qquad t^* = t\omega^{-1} \quad \text{(A3)}$$

$$(x^*, y^*) = L_0(x, y),$$

where ω is the dominant frequency of the tidal wave, L_0 is a spatial scale describing the planimetric variations of the flow characteristics, D_0 denotes a typical value of the maximum flow depth which can be reached on the salt marsh during over-bank spring tides, U_0 is a characteristic value of the depth-averaged flow velocity, and a_0 is the typical scale of spatial variations in water surface elevation from the channels to the watershed divide.

Substitution of (A3) into (A1a), (A1b), and (A1c) leads to the following dimensionless form of momentum and continuity equations:

$$S\frac{\partial U}{\partial t} + SF\left[U\frac{\partial U}{\partial x} + V\frac{\partial U}{\partial y}\right] + \frac{\partial \eta_1}{\partial x} + R\frac{U}{D}\sqrt{U^2 + V^2} = 0 \quad \text{(A4a)}$$

$$S\frac{\partial V}{\partial t} + SF\left[U\frac{\partial V}{\partial x} + V\frac{\partial V}{\partial y}\right] + \frac{\partial \eta_1}{\partial y} + R\frac{V}{D}\sqrt{U^2 + V^2} = 0 \quad \text{(A4b)}$$

$$\frac{\partial D}{\partial t} + F\left[\frac{\partial (UD)}{\partial x} + \frac{\partial (VD)}{\partial y}\right] = 0 \quad \text{(A4c)}$$

where

$$D(x, y, t) = \eta_0(t) + \varepsilon\eta_1(x, y, t) - z(x, y) \quad \text{(A5)}$$

and the nondimensional parameters S, F, R, and ε read

$$F = \frac{U_0}{\omega L_0}, \qquad S = \frac{\omega U_0 L_0}{g a_0}, \qquad R = \frac{L_0 U_0^2}{C^2 D_0 a_0}, \qquad \varepsilon = \frac{a_0}{D_0}. \quad \text{(A6)}$$

In particular, the parameters S and R in momentum equations denote a measure of the effect of local inertia and friction, respectively, relative to that of gravity. It is worth noting that the ratio $S/R = (C^2 D_0 \omega)/(gU_0)$ is independent on the length scale L_0 and on the typical spatial variation of surface elevation a_0. Field data on the ratio S/R show that $S/R \ll 1$; hence the flow on salt marshes and creeks is frictionally dominated [e.g., *Friedrichs and Madsen*, 1992]. To ensure the mass balance in the continuity equation, we set $F = 1$, which allows us to estimate the length scale L_0. On the basis of data reported in Table A1, the resulting values, ranging from ~300 to 700 m, are consistent with the average path of a water particle on the salt marsh. Moreover, from the balance of momentum equations we can set $R = 1$ thus yielding

$$\frac{a_0}{L_0} = \frac{U_0^2}{C^2 D_0}, \quad \text{(A7)}$$

whence the resulting estimates of water surface slope on the creek network and on the salt marsh are $O(10^{-5})$ and $O(10^{-4})$ respectively, and are in good agreement with available field data [*Healey et al*., 1981; *French and Stoddart*, 1992]. Therefore on the basis of the above estimates a balance between water surface slope and friction is likely to hold in momentum equations, which allows one to write

$$\frac{\partial \eta_1}{\partial x} = -\Lambda\frac{U}{D}, \qquad \frac{\partial \eta_1}{\partial y} = -\Lambda\frac{V}{D}, \quad \text{(A8)}$$

where, for the sake of simplicity, the friction term has been linearized by using the energy criterion first introduced by *Lorentz* [1926] [see, e.g., *Zimmerman*, 1982; *Jay*, 1991], that is, by setting

$$\frac{U}{D}\sqrt{U^2 + V^2} \sim \Lambda\frac{U}{D}, \qquad \frac{V}{D}\sqrt{U^2 + V^2} \sim \Lambda\frac{V}{D}, \quad \text{(A9)}$$

with Λ being an effective friction coefficient, which depends on a characteristic velocity scale $\propto \sqrt{U_2 + V^2}$. In practice, one uses a uniform Λ thought proportional to the velocity scale U_0.

We note that (A9) is appropriate for analysis of the integral properties of a tidal basin (such as delineation of drainage divides) but not for the determination of the exact velocity distribution [*Zimmerman*, 1982]. Even when the tidal system is frictionally dominated, the linearization of the friction term might cause an incorrect prediction of velocity and surface elevation asymmetries throughout the tidal cycle [*Lanzoni and Seminara*, 1998].

Substituting (A8) into (A4c) and recalling the dimensionless water depth decomposition (A5) yields

$$\frac{\partial}{\partial t}(\eta_0 + \varepsilon\eta_1 - z) - \frac{1}{\Lambda}\left\{\frac{\partial}{\partial x}\left[(\eta_0 + \varepsilon\eta_1 - z)^2\frac{\partial \eta_1}{\partial x}\right] + \frac{\partial}{\partial y}\left[(\eta_0 + \varepsilon\eta_1 - z)^2\frac{\partial \eta_1}{\partial y}\right]\right\} = 0. \quad \text{(A10)}$$

The parameter ε, in general, is not necessarily small. Nevertheless, it is likely to be small for relatively short embayments, where the salt marsh area is small enough to ensure a relatively fast propagation and a weak deformation of the tidal wave. Hence neglecting in (A10) the terms of order $O(\varepsilon)$ and

Table A1. Scales and Nondimensional Parameters

	U_0, m/s	D_0, m	C, $m^{1/2}/s$	a_0/L_0	S/R
Creeks	0.5 ÷ 0.7	2 ÷ 3	30 ÷ 40	$\sim 10^{-5}$	~0.1
Salt marsh surface	0.05 ÷ 0.1	0.2 ÷ 0.3	10 ÷ 20	$\sim 10^{-4}$	~0.01

Sources are as follows: *Myrick and Leopold* [1963], *Bayliss-Smith et al*. [1978], *Healey et al*. [1981], *French and Stoddart* [1992], *Lynn et al*. [1995], and *Shi et al*. [1995].

assuming, for the sake of simplicity, a nearly flat salt marsh bottom (i.e., $z(x, y) \approx z_b$), we find

$$\nabla^2 \eta_1 = \frac{\Lambda}{(\eta_0 - z_b)^2} \frac{\partial \eta_0}{\partial t}. \quad \text{(A11)}$$

This approximation holds only when the water depth over the salt marshes is high enough to ensure that $\eta_0 \gg \varepsilon \eta_1$. We can then use (A11) to draw the water surface across the marsh at high water and, through (A8), to design a steepest descent method to delineate flow directions.

Equation (A11) needs boundary conditions to be specified at the three different morphological borders limiting the salt marsh surface, namely, the mainland, the salt marsh edge, and the creeks. At the boundary with the mainland we apply the classical requirement of no flux in the direction n normal to the boundary (i.e., $\partial \eta_1 / \partial n = 0$). We also assume that the water level on the tidal flats bordering the salt marsh and in the creeks dissecting it is spatially independent and equal to $\eta_0(t)$ (i.e., we impose $\eta_1 = 0$). The tidal wave, in fact, travels much faster along the creek network than on salt marshes, its celerity being proportional to the square root of flow depth. As shown in Table A1, a_0/L_0 is about 10^{-5}, which means that tidal surface is essentially horizontal along the creek system during the flood part of the tidal cycle [*Healey et al*., 1981], and the water surface slope in the creeks is about an order of magnitude smaller than that on salt marshes. The assumption of a horizontal water surface in the smaller channels where flow depth is only slightly larger than on the salt marshes, however, is probably less correct.

Finally, in order to derive time-independent solutions, we assume reasonable values of the quantities $\eta_0(t)$ and $\partial \eta_0 / \partial t$ appearing on the left side of (A10). Preliminary calculations, in fact, showed that fairly large variations of the term $K = \Lambda/(\eta_0 - z_b)^2 \partial \eta_0 / \partial t$ cause relatively small differences in flow directions and therefore in divide delineation. For a given salt marsh domain Γ, the analytical problem can thus be formulated as the solution of the Poisson equation $\nabla^2 \eta_1 = K$ subject to the boundary conditions $\partial \eta_1 / \partial n = 0$ or $\eta_1 = 0$ on $\partial \Gamma$.

Acknowledgments. Funds provided by MURST 40% and the University of Padua through the projects Trasporto di sedimenti ed evoluzione morfologica di corsi d'acqua, estuari e lagune alle diverse scale temporali and Morfodinamica Fluviale e Costiera (1999/048/2/14/05/001) are gratefully acknowledged. The paper greatly benefited from a thorough review by Chris Paola and an anonymous reviewer and from discussions with Riccardo Rigon and Ignacio Rodriguez-Iturbe.

References

Bayliss-Smith, T. P., R. Healey, R. Lailey, T. Spencer, and D. R. Stoddart, Tidal flows in salt-marsh creeks, *Estuarine Coastal Mar. Sci*., *9*, 235–255, 1978.

Boon, J. D., III, Tidal discharge asymmetry in a salt marsh drainage system, *Limnol. Oceanogr*., *20*, 71–80, 1975.

Boon, J. D., and R. J. Byrne, On basin hypsometry and the morphodynamic response of coastal inlet systems, *Mar. Geol*., *40*, 27–48, 1981.

Collins, L. M., J. M. Collins, and L. B. Leopold., Geomorphic processes of an estuarine marsh: Preliminary results and hypothesis, in *International Geomorphology, 1986: Proceedings of the First International Conference on Geomorphology*, vol. 1, edited by V. Gardiner, pp. 1049–1071, John Wiley, New York, 1987.

Dronkers, J. J., *Tidal Computations in Rivers and Coastal Waters*, North-Holland, New York, 1964.

Fagherazzi, S., A. Bortoluzzi, W. E. Dietrich, A. Adami, S. Lanzoni, M. Marani, and A. Rinaldo, Tidal networks, 1, Automatic network extraction and preliminary scaling features from digital terrain maps, *Water Resour. Res*., this issue.

French, J. R., and D. R. Stoddart, Hydrodynamics of salt marsh creek systems: Implications for marsh morphological development and material exchange, *Earth Surf. Processes Landforms*, *17*, 235–252, 1992.

Friedrichs, C. T., Stability, shear stress and equilibrium cross-sectional geometry of sheltered tidal channels, *J. Coastal Res*., *11*(4), 1062–1074, 1995.

Friedrichs, C. T., and O. S. Aubrey, Nonlinear tidal distortion in shallow well-mixed estuaries: A synthesis, *Estuarine Coastal Shelf Sci*., *27*, 521–545, 1988.

Friedrichs, C. T., and O. S. Madsen, Nonlinear diffusion on the tidal signal in frictionally dominated embayments, *J. Geophys. Res*., *97*, 5637–5650, 1992.

Grey, D. M., Interrelationships of watershed characteristics, *J. Geophys. Res*., *66*, 1215–1223, 1961.

Hack, J. T., Studies of longitudinal profiles in Virginia and Maryland, *U.S. Geol. Surv. Prof. Pap*., *294-B*, 1957.

Healey, R. G., K. Pye, D. R. Stoddart, and T. P. Bayliss-Smith, Velocity variation in salt marsh creeks, Norfolk, England, *Estuarine Coastal Shelf Sci*., *13*, 535–545, 1981.

Jay, D. A., Green's law revisited: Tidal long-wave propagation in channels with strong topography, *J. Geophys. Res*., *96*, 20,585–20,598, 1991.

Kirchner, J. W., Statistical inevitability of Horton's laws and the apparent randomness of stream channel networks, *Geology*, *21*, 591–594, 1993.

Kirkby, M. J., Tests of the random model and its application to basins hydrology, *Earth Surf. Processes Landforms*, *1*, 197–212, 1976.

Lanzoni, S., and G. Seminara, On tide propagation in convergent estuaries, *J. Geophys. Res*., *103*, 30,793–30,812, 1998.

Leopold, L. B., L. Collins, and M. Inbar, Channel and flow relationships in tidal salt marsh wetlands, *Tech. Rep. G830-06*, 78 pp., Calif. Water Resour. Cent., U.S. Geol. Surv., Davis, 1984.

Leopold, L. B., J. N. Collins, and L. M. Collins, Hydrology of some tidal channels in estuarine marshlands near San Francisco, *Catena*, *20*, 469–493, 1993.

Lorentz, H. A., Verslag Staatcommissie Zuiderzee 1918–1926, *Rep. Govt. Zuiderzee Comm*., Alg. Landsddrukkerij, Den Haag, 1926.

Lynn, A. L., A. C. Hine, and M. E. Luther, Surficial sediment transport and deposition processes in a *Juncus roemerianus* marsh, west-central Florida, *J. Coastal Res*., *11*, 322–336, 1995.

Mandelbrot, B. B., *The Fractal Geometry of Nature*, W. H. Freeman, New York, 1982.

Marani, M., A. Rinaldo, R. Rigon, and I. Rodriguez-Iturbe, Geomorphological width functions and the random cascade, *Geophys. Res. Lett*., *21*(19), 2123–2126, 1994.

Marani, M., J. R. Banavar, G. Caldarelli, A. Maritan, and A. Rinaldo, Stationary self-organized fractal structures in an open, dissipative electrical system, *J. Phys. A Math. Gen*., *31*, 337–343, 1998.

Montgomery, D. R., and W. E. Dietrich, Where do channels begin?, *Nature*, *336*, 232–234, 1988.

Montgomery, D. R., and W. E. Dietrich, Channel initiation and the problem of landscape scale, *Science*, *255*, 826–830, 1992.

Muller, J. E., Re-evaluation of the relationship of master streams and drainage basins: Reply, *Geol. Soc. Am. Bull*., *84*, 3127–3130, 1973.

Myrick, R. M., and L. B. Leopold, Hydraulics geometry of a small tidal estuary, *U.S. Geol. Surv. Prof. Pap*., *422-B*, 18 pp., 1963.

Parker, B. B., The relative importance of various nonlinear mechanisms in a wide range of tidal interactions, in *Tidal Hydrodynamics*, edited by B. B. Parker, pp. 237–268, John Wiley, New York, 1991.

Pestrong, R., The development of drainage patterns on tidal marshes, *Stanford Univ. Publ. Geol. Sci*., *10*, 87 pp., 1965.

Pethick, J. S., Velocity surges and asymmetry in tidal channels, *Estuarine Coastal Mar. Sci*., *11*, 331–345, 1980.

Rigon, R., I. Rodriguez-Iturbe, A. Rinaldo, A. Giacometti, A. Maritan, D. Tarboton, and A. Rinaldo, On Hack's law, *Water Resour. Res*., *32*, 3367–3374, 1996.

Rinaldo, A., W. E. Dietrich, R. Rigon, G. K. Vogel, and I. Rodriguez-Iturbe, Geomorphological signatures on varying climate, *Nature*, *374*, 632–636, 1995.

Rinaldo, A., I. Rodriguez-Iturbe, and R. Rigon, Channel networks, *Annu. Rev. Earth Planet Sci*., *26*, 289–327, 1998.

Rinaldo, A., S. Fagherazzi, S. Lanzoni, M. Marani, and W. E. Dietrich,

Tidal networks, 3, Landscape-forming discharges and studies in empirical geomorphic relationships, *Water Resour. Res*., this issue.

Rodriguez-Iturbe, I., and A. Rinaldo, *Fractal River Basins: Chance and Self-Organization*, Cambridge Univ. Press, New York, 1997.

Shuttelaars, H. M., and H. E. De Swart, An idealized long-term morphodynamic model of a tidal embayment, *Eur. J. Mech. B Fluids*, *15*(1), 55–80, 1996.

Shi, Z., J. S. Pethick, and K. Pye, Flow structure in and above the various heights of a salt marsh canopy, a laboratory flume study, *J. Coastal Res*., *11*, 1204–1209, 1995.

Speer, P. E., and D. G. Aubrey, A study of non-linear tidal propagation in shallow inlet/estuarine systems, II, Theory, *Estuarine Coastal Shelf Sci*., *21*, 207–224, 1985.

Steel, T. J., and K. Pye, The development of salt marsh tidal creek networks: Evidence from the UK, paper presented at Canadian Coastal Conference, Can. Coastal Sci. and Eng. Assoc., Guelph, Ont., May 21–24, 1997.

Tarboton, D. G., R. L. Bras, and I. Rodriguez-Iturbe, The fractal nature of river networks, *Water Resour. Res*., *24*, 1317–1322, 1988.

Van Dongeren, A. R., and H. J. De Vriend, A model of morphological behaviour of tidal basins, *Coastal Eng*., *22*, 287–310, 1994.

Zimmermann, J. T. F., On the Lorentz linearization of a quadratically damped forced oscillator, *Phys. Lett*., *A89*,(3), 123–124, 1982.

W. E. Dietrich, Department of Geology and Geophysics, University of California, Berkeley, Berkeley, CA 94720. (bill@geomorph.berkeley.edu)

S. Fagherazzi, Computational Science and Engineering Program, Florida State University, Tallahassee, FL 32306. (sergio@cse.fsu.edu)

S. Lanzoni, M. Marani, and A. Rinaldo, Dipartimento di Ingegneria Idraulica, Marittima e Geotecnia, Universitá di Padova, via Loredan 20, I-35131 Padua, Italy. (lanzo@idra.unipd.it; marani@idra.unipd.it; rinaldo@idra.unipd.it)

(Received August 5, 1998; revised July 16, 1999;
accepted July 21, 1999.)